

1
2
3
4
5
6
7
8
9
10
11
12
13
14
15
16
17
18
19
20
21
22

**The division inhibitor EzrA contains a seven-residue patch required
for maintaining the dynamic nature of the medial FtsZ ring**

Daniel P. Haeusser, Anna Cristina Garza, Amy Z. Buscher and Petra Anne Levin *

Department of Biology, Washington University, St. Louis, MO 63130, USA

Running Title: Structure-Function Analysis of EzrA

*Corresponding Author

Tel. 314-935-7888

Fax 314-935-4432

Email: plevin@biology.wustl.edu

1 **ABSTRACT**

2 The essential cytoskeletal protein FtsZ assembles into a ring-like structure at the nascent
3 division site and serves as a scaffold for the assembly of the prokaryotic division machinery. We
4 previously characterized EzrA as an inhibitor of FtsZ assembly in *Bacillus subtilis*. EzrA
5 interacts directly with FtsZ to prevent aberrant FtsZ assembly and cytokinesis at cell poles. EzrA
6 also concentrates at the cytokinetic ring in an FtsZ-dependent manner, although its precise role at
7 this position is not known. Here, we identify a conserved patch of amino acids in the EzrA C-
8 terminus that is essential for localization to the FtsZ ring. Mutations in this patch (termed here
9 the “QNR patch”) abolish EzrA localization to midcell, but do not significantly affect EzrA’s
10 ability to inhibit FtsZ assembly at cell poles. *ezrA* QNR mutants exhibit stabilized FtsZ assembly
11 at midcell and are significantly longer than wild type cells, despite lacking extra FtsZ rings.
12 These results indicate that EzrA has two distinct activities *in vivo*: 1) preventing aberrant FtsZ
13 ring formation at cell poles through inhibition of *de novo* FtsZ assembly, and 2) maintaining
14 proper FtsZ assembly dynamics within the medial FtsZ ring, thereby rendering it sensitive to the
15 factors responsible for coordinating cell growth and cell division.

16
17
18
19
20
21
22
23

1 INTRODUCTION

2 At the onset of cell division, the tubulin-like FtsZ protein assembles into a membrane-
3 associated ring that establishes the division site in most bacteria and archaea, as well as in
4 chloroplasts and the mitochondria of certain protists (21). The FtsZ ring is present for a large
5 portion of the cell cycle (the Z-period), serving as a scaffold for assembly of the division
6 apparatus and constricting at the leading edge of the invaginating septum at the onset of division
7 (10).

8 Like tubulin, FtsZ assembly dynamics derive from GTP binding and hydrolysis. *In vitro*
9 GTP binding induces FtsZ assembly into single-stranded polymers. These polymers then interact
10 laterally to form the bundles (19, 23) that are thought to constitute the FtsZ ring *in vivo* (21, 25).
11 Subsequent GTP hydrolysis destabilizes FtsZ polymers, which become curved and rapidly
12 disassemble (25).

13 In the cell, FtsZ exists in a precise balance between the membrane-associated single-
14 stranded polymers and bundles that constitute the FtsZ ring and the cytoplasmic monomers and
15 small multimers that constitute the pool of FtsZ subunits available for exchange into the
16 cytokinetic ring (21, 25). Disturbances in FtsZ assembly dynamics result in aberrant division
17 events or potentially lethal filamentation (10, 21, 25). The FtsZ ring itself is a highly dynamic
18 structure. Fluorescence recovery after photo-bleaching (FRAP) experiments indicate that the
19 half-life of an individual subunit is between 4 and 20 seconds (1). Maintaining the precise
20 balance between FtsZ assembly and disassembly is critical for coordinating division with cell
21 growth and to ensure that daughter cells each receive a full genetic complement following
22 cytokinesis (10, 21, 25).

1 FtsZ levels are constant throughout the cell cycle and the spatial and temporal control of
2 division is governed primarily at the level of FtsZ assembly (30). To date, a handful of proteins
3 have been identified that modulate FtsZ assembly dynamics *in vivo* (6, 10). One of these, EzrA,
4 is an inhibitor that prevents aberrant FtsZ assembly at the poles of exponentially growing cells
5 (8, 17, 19).

6 EzrA is found throughout the low-GC Gram-positive bacteria and exhibits significant
7 structural conservation. EzrA is anchored in the plasma membrane by an N-terminal
8 transmembrane domain. The remainder of the EzrA polypeptide consists of a series of predicted
9 cytoplasmic coiled coil domains (17). This somewhat unusual topology (N-terminal out) is
10 shared with ZipA, a cell division protein that is found in the gamma subdivision of the
11 proteobacteria (9). Null mutations in *ezrA* lower the concentration of FtsZ required for assembly
12 *in vivo*, leading to the formation of polar FtsZ rings and septa (17) and stabilizing FtsZ assembly
13 at midcell (19).

14 A purified Thioredoxin-EzrA fusion lacking the EzrA transmembrane anchor (Thio-
15 EzrA) interacts with FtsZ *in vitro* and inhibits FtsZ assembly in both sedimentation and 90°
16 angle light scattering assays (8). Deletion analysis indicates that EzrA interacts with the C-
17 terminal sixteen residues of FtsZ to inhibit assembly *in vitro* (28). It has recently been reported
18 that the addition of the native cytoplasmic portion of EzrA results in a modest (1.6-fold) increase
19 in FtsZ GTP hydrolysis (5), suggesting that EzrA may increase subunit turnover. However, the
20 precise mechanism by which EzrA modulates FtsZ ring formation remains unknown, as an EzrA
21 fusion protein lacking the transmembrane domain effectively inhibits FtsZ assembly *in vitro*
22 without altering FtsZ's intrinsic GTPase activity (8).

1 EzrA exhibits two distinct patterns of subcellular localization. In pre-divisional cells
2 EzrA is uniformly distributed throughout the plasma membrane. Paradoxically, given its ability
3 to inhibit FtsZ assembly, EzrA also concentrates at the division site in an FtsZ-dependent manner
4 (17). EzrA's role at midcell is unclear. EzrA localization to the medial ring may simply be a
5 consequence of residual interaction with FtsZ. Alternatively, EzrA may promote subunit
6 turnover at midcell. Arguing against this latter model, FRAP experiments on FtsZ rings indicate
7 little change in subunit turnover in the absence of EzrA (1). However, cells lacking EzrA are
8 significantly longer than wild type cells (4, 14, 17), consistent with altered FtsZ assembly
9 dynamics at midcell that disrupt the coupling of division with cell growth.

10 To clarify the role of EzrA at midcell, we have employed a combination of deletion
11 analysis and site-directed mutagenesis to identify regions of EzrA that are required for medial
12 localization. Using this approach we have identified a conserved 7-residue patch (termed the
13 "QNR patch" after the three most conserved residues) that is required for EzrA localization to
14 the FtsZ ring. A single substitution in the QNR patch abolishes medial EzrA localization but
15 does not alter the ability of EzrA to inhibit FtsZ assembly *in vitro*, and only results in a
16 negligible increase in polar FtsZ assembly. However, despite lacking extra FtsZ rings, *ezrA* QNR
17 mutants are longer than their wild type counterparts and exhibit stabilized FtsZ assembly at
18 midcell, similar to an *ezrA* null mutant. Together, our results support a model in which EzrA
19 serves two distinct functions *in vivo*: 1) preventing aberrant FtsZ ring formation by inhibiting *de*
20 *novo* FtsZ assembly at cell poles and 2) maintaining proper FtsZ assembly dynamics within the
21 medial FtsZ ring.

22
23

1 MATERIALS AND METHODS

2 *General methods and strain construction*

3 Strains are listed in Table 1. All *B. subtilis* strains are derivatives of JH642 (24). Cloning
4 and genetic manipulation were performed using standard techniques (11, 26). The *E. coli* strain
5 AG1111 (12) was used for plasmid construction, unless otherwise noted. Vent DNA polymerase
6 (NEB) or KlentaqLA (DNA Polymerase Technology, Inc.) were used for polymerase chain
7 reactions (PCRs). All oligonucleotide sequences and plasmid information are available upon
8 request.

9 Luria-Bertani (LB) media was used unless otherwise noted, and cells were grown at 37°C
10 for strains bearing the wild-type *ftsZ* allele or 30°C for strains bearing the heat-sensitive *ftsZts*
11 (*ftsZ-gfp*) allele. Chloramphenicol (Sigma) was used at a final concentration of 5 µg/mL,
12 spectinomycin (Sigma) at 100 µg/mL, kanamycin (EM Sciences) at 10 µg/mL, and ampicillin
13 (Fisher Scientific) at 100 µg/mL. Strains resistant to macrolides, lincosamides, and
14 streptogramins (MLS) were cultured in media containing erythromycin (Fisher Scientific) at a
15 final concentration of 0.5 µg/mL and lincomycin (ICM Biomedicals) at 2.5 µg/mL. Isopropyl-β-
16 D-thiogalactopyranoside (IPTG) (Sigma) was used at 1 mM.

17 The *eZR*A::*kan* null mutation was created by inserting a 1.4 kb kanamycin cassette
18 between codons 147 and 285 of *eZR*A. The *kan* cassette was removed from pGK67 (15) by
19 *Sma*I/*Pst*I (NEB) digestion and ligated into a 1.1 kb *eZR*A fragment within a derivative of pCR2.1
20 (Invitrogen) digested with *Pst*I/*Eco*47III (NEB). The resulting plasmid was transformed into
21 JH642 for *eZR*A::*kan* integration at the native *eZR*A locus by double-crossover homologous
22 recombination, selecting for kanamycin resistance. Proper integration was verified by PCR.

1 C-terminal EzrA truncations that are fused to GFP were created in pPL65 [a derivative of
2 pUS19 (2) containing an ~900 bp 3' *ezrA* fragment fused to *gfp*]. The wild-type *ezrA* fragment
3 was cut from the vector by *EcoRI/XhoI* (NEB) digestion and replaced with a relevant *ezrA*-
4 truncation fragment amplified by PCR from JH642 chromosome. All *ezrA-gfp* point mutations
5 and the *ezrAΔ501-511-gfp* deletion were created using the QuikChange® Site-Directed
6 Mutagenesis Kit (Stratagene) on pPL65. Tagless mutants lacking GFP were constructed by PCR
7 amplification of the *ezrA* fragment (residues 355-562) with *EcoRI/BamHI* (NEB) linkers from
8 the pPL65-derivatives and placing them into pUS19. The resulting plasmids were transformed
9 into JH642, selecting for single-crossover recombination events at the native *ezrA* locus by
10 growth on spectinomycin-containing media. Mutations were confirmed by plasmid sequencing
11 and integration was confirmed by chromosomal *ezrA* locus sequencing.

12 Strains for the *minCD* and *ftsZts* suppression assays were constructed by transforming
13 chromosome from the tagless *ezrA* mutant strains into the relevant background and selecting for
14 the appropriate antibiotic resistance. *minCD* and *ftsZts* suppression assays were conducted as
15 previously described (19, 31).

16 The Thio-EzrAΔTM(R510D)-6XHis fusion [Thio-EzrA(R510D)] under P_{bad} control (7)
17 was constructed by amplification of full length *ezrAΔTM(R510D)* from PL1780, followed by
18 TOPO cloning (Invitrogen) as described previously for the wild type EzrA fusion (Thio-EzrA)
19 (8). After verifying the mutation within the plasmid by sequencing, the plasmid was transformed
20 into 'One Shot chemically competent' TOP10 cells (Invitrogen), and then isolated and
21 transformed into a BB101 background (3) for protein induction and purification.

22

23

1 **Microscopy**

2 Fluorescence microscopy was performed as described (17). An Olympus BX51
3 microscope with Chroma filters and a Hamamatsu OrcaERG camera were used for image
4 capture. Images were processed using Openlab version 5.0.1 (Improvision) and Adobe
5 Photoshop CS version 8.0 (Adobe Systems). All cell or ring measurements from collected
6 images were done with a minimum population of 200 cells/strain.

7 GFP fusions were visualized in live cells as described (16). Briefly, cells grown to mid-
8 exponential phase ($OD_{600} \sim 0.4$) in liquid culture were stained with the vital membrane dye FM
9 4-64 (Invitrogen) at a dilution of 1:2000 for one to three minutes and then placed on 1% agarose
10 in 1X PBS pads (16) on glass microscope slides. EzrA-GFP localization to midcell was scored as
11 strong, weak, or none based on fluorescent band intensity. Statistical analysis of EzrA-GFP
12 localization between strains was performed using a χ^2 test with 2 degrees of freedom (df) and a
13 significance (α) of 0.001.

14 Cells were prepared for immunofluorescence microscopy by paraformaldehyde and
15 gluteraldehyde treatment, as described previously (16, 17), with lysozyme incubation typically
16 lasting seven to ten minutes. FtsZ was detected using affinity-purified polyclonal rabbit anti-FtsZ
17 sera (18) in combination with donkey anti-rabbit sera conjugated to Cyanine-3 (Jackson
18 Immunoresearch). Cell walls were visualized with wheat germ agglutinin (WGA) conjugated to
19 fluorescein (Invitrogen). Statistical analysis of FtsZ localization between strains was performed
20 using a χ^2 test (df = 5 and $\alpha = 0.001$).

21 Cell lengths were measured with fixed cells, using a three to four minute lysozyme
22 treatment that better preserved cell wall structure. Septa were defined as bands of fluorescent
23 signal that fully traversed the cell width with intensity equal to or greater than lateral wall

1 fluorescence. Cell length data was obtained with Openlab software and exported to Microsoft
2 Excel (version 11.1) for analysis. Statistical analysis of cell lengths between strains was
3 performed using a χ^2 test (df = 5 and $\alpha = 0.001$). Length to ring ratios were determined as
4 described (29, 32).

6 ***Protein Purification***

7 *B. subtilis* FtsZ was purified from PL1184, an *E. coli* ER2566 derivative, as described (8,
8 31). Thio-EzrA and Thio-EzrA(R510D) were purified from *E. coli* BB101 (3) derivatives
9 (PL1364 and PL1821, respectively) as described (8). A size exclusion chromatography step was
10 added to our original protocol to remove EzrA degradation products that frequently caused
11 aggregation and precipitation of the final product.

12 One-liter cultures of cells containing induced Thio-EzrA or Thio-EzrA(R510D) were
13 pelleted, washed in EzrA Induction Buffer (50 mM NaPO₄, pH 8.0, 300 mM NaCl), repelleted
14 and frozen at -80°C for later use. On the day of purification, cell pellets were thawed and
15 resuspended in 30 mL of ice cold EzrA Induction Buffer + 1 mM 4-(2-Aminoethyl)
16 benzenesulfonyl fluoride hydrochloride (AEBSF) (Sigma). Cells were lysed by two to three
17 passes in a pre-chilled, 30 mL-capacity French Press cell at 1000 psi. All subsequent steps were
18 performed at 4°C. Lysates were cleared by centrifugation as described (8) and loaded in EzrA
19 Buffer 350 (50 mM HEPES pH 7.5, 350 mM NaCl) + 50 mM imidazole onto two tandem 5 mL
20 Hi-Trap chelating HP columns (GE Healthcare) charged with nickel on an ÄKTA prime low-
21 pressure purification system (GE Healthcare). Bound EzrA was washed with EzrA Buffer 350 +
22 75 mM imidazole and bound protein was eluted in one step with EzrA Buffer 350 + 200 mM
23 imidazole. Peak fractions were pooled, concentrated to ~1 – 2 mL using Centricon YM-50 filters

1 (Fisher Scientific), and applied to an S300 gel filtration column (GE Healthcare) pre-equilibrated
2 with EzrA Buffer 175 (50 mM HEPES, pH 7.5, 175 mM NaCl, 1 mM EGTA). Both Thio-EzrA
3 and Thio-EzrA(R510D) proteins eluted in three peaks: a small inactive aggregate peak, an active
4 peak with the apparent molecular weight of a dimer, and an inactive peak with the apparent
5 molecular weight of a monomer. Fractions from the active peak were collected, pooled and
6 concentrated with YM-50 filters. Glycerol was added to 10% final concentration and aliquots
7 were flash frozen at -80°C .

8 FtsZ protein concentration was determined by an average of BCA (Pierce) and
9 Coomassie Plus (Pierce) assay estimates, while EzrA fusion concentrations were estimated by
10 BCA and Coomassie Plus assays, as well as by A_{280} (molar extinction coefficient = 58656.0
11 A_{280}/mole as determined by Gene Inspector, version 1.6.3, Textco) using a SPECTRAmax Plus
12 (Molecular Devices) spectrophotometer.

14 ***90° angle light scattering assay***

15 Light scattering assays were conducted essentially as described (8, 31) using a DM-45
16 spectrofluorimeter (Olis). Readings were taken four times per second at 30°C , and a baseline was
17 gathered for 1 minute before the addition of 1 mM GTP to the cuvette. Reactions contained 5 μM
18 FtsZ diluted in Polymerization Buffer (50 mM MES pH 6.5, 2.5 mM $\text{Mg}(\text{CH}_3\text{COO}^-)_2$, 1 mM
19 EGTA, 50 mM KCH_3COO^-) and EzrA Buffer 175 + 10% glycerol with or without Thio-EzrA or
20 Thio-EzrA(R510D). Data was collected by SpectralWorks (Olis), and exported into Microsoft
21 Excel for data processing. Baseline corrections were applied in Excel to remove background
22 signal from unassembled FtsZ and the EzrA fusions.

23

1 RESULTS

2 A conserved seven-residue patch is required for EzrA localization to the FtsZ ring.

3 To clarify the role of EzrA at midcell, we undertook a structure-function analysis of
4 EzrA. Sequence alignment across fourteen species predicts a conserved EzrA domain structure
5 (Figure 1A) of an amino-terminal transmembrane anchor and a series of cytoplasmic coiled coils
6 that vary in length and number between species. While primary sequence conservation is
7 generally poor, EzrA contains a well-conserved patch of 7 amino acids near its C-terminus (the
8 “QNR patch”). In *B. subtilis*, the QNR patch lies just after the fourth coiled-coil, residues 505-
9 511: IQFGNRF (Figure 1B).

10 We constructed a series of nested deletions in a functional, full-length EzrA-GFP fusion
11 in order to identify regions essential for localization to the FtsZ ring (Figure 1C). All *ezrA-GFP*
12 mutant constructs were expressed from the native *ezrA* promoter and were the only copy of *ezrA*
13 in the cell (see Materials and Methods). Full length EzrA-GFP localizes throughout the plasma
14 membrane and concentrates at midcell in an FtsZ-dependent manner (17). In contrast, EzrA-GFP
15 deletions that were missing residues up to and including the fourth coiled coil (Figure 1C) all
16 failed to localize to midcell, but retained association with the plasma membrane (Figure 2A).
17 However, EzrA Δ 551-562-GFP, a comparatively small C-terminal truncation, showed the same
18 localization as full length EzrA-GFP (Figure 2A).

19 These results suggest that the sequence determinant for EzrA localization to the FtsZ ring
20 lies within residues 501-550: a region that contains the QNR patch. In confirmation of this
21 hypothesis, a fusion lacking the QNR patch was unable to localize to the FtsZ ring (Figure 2B),
22 indicating that these residues are required for medial EzrA localization.

1 We next employed site-directed mutagenesis to identify specific residues within the QNR
2 patch that are required for medial EzrA localization. For these experiments, we targeted the three
3 most conserved residues for alanine substitution: Q506, N509, and R510. We also constructed an
4 R510D charge-reversal (Figure 1C).

5 Fluorescence microscopy of live cells expressing various EzrA-GFP fusions indicated
6 that single substitutions in the QNR patch disrupted EzrA localization to the FtsZ ring, albeit to
7 differing degrees (Figure 2B and Table 2). The majority of *ezrA-gfp* cells displayed strong
8 medial EzrA localization (Figure 2A and Table 2). In contrast, cells encoding *ezrA(Q506A)-gfp*
9 had a two-fold decrease in the population exhibiting strong medial EzrA localization and a
10 corresponding increase in weak localization (Figure 2B and Table 2). This phenotype was more
11 pronounced in *ezrA(N509A)-gfp* and *ezrA(R510A)-gfp* cells, where the majority (60-67%)
12 showed no medial EzrA localization (Figure 2B and Table 2). Notably, EzrA localization to the
13 FtsZ ring was completely abolished in *ezrA(R510D)-gfp* cells (Figure 2B and Table 2).

14 The loss of EzrA-GFP localization to midcell through truncations or point mutations was
15 not due to altered EzrA or FtsZ expression. Quantitative immunoblotting indicated that the EzrA-
16 GFP fusion proteins were the expected size, were expressed at levels comparable to full length
17 EzrA-GFP, and did not alter FtsZ levels (data not shown). Together, these results indicate that
18 the QNR patch is essential for EzrA localization to the FtsZ ring.

19 20 **Mutations in EzrA's QNR patch stabilize FtsZ assembly at midcell.**

21 Loss of EzrA stabilizes FtsZ assembly at midcell (17, 19), suggesting that EzrA plays an
22 active role at this position. To test this possibility, we examined the effect of mutations in EzrA's
23 QNR patch on the lethality associated with overexpression of the division inhibitor MinCD.

1 During exponential growth the MinCD complex is involved in preventing inappropriate FtsZ
2 ring formation at cell poles (20, 22); however, >12-fold overexpression of MinCD shifts the
3 cellular balance of FtsZ dynamics towards unassembled FtsZ, blocking FtsZ ring formation and
4 causing lethal filamentation in *B. subtilis* (20, 22). Stabilizing FtsZ assembly at midcell via a
5 mutation in a division inhibitor such as *ezrA* permits FtsZ ring formation and division even in the
6 presence of excess MinCD (19, 29, 31).

7 For these experiments we cloned the four *ezrA* QNR point mutants (Figure 1C, bottom)
8 under the control of the native *ezrA* promoter, and without GFP tags, into otherwise wild type
9 cells. Each *ezrA* QNR mutant was then transformed into a strain encoding an IPTG-inducible
10 *minCD* overexpression construct: *P_{spachy}-minCD*. Viability was tested by plating cells onto
11 medium containing 1 mM IPTG to induce >12-fold overexpression of MinCD. Removal of the
12 GFP tag did not alter *EzrA* mutant stability or expression and FtsZ levels were wild type in all
13 strain backgrounds (data not shown).

14 Suppression of MinCD-induced lethality by mutations in *ezrA*'s QNR patch (Figure 3A)
15 correlated with the ability of individual QNR mutants to localize to the FtsZ ring (Figure 2B). As
16 expected, viability was reduced ~28,000-fold following MinCD overexpression in *ezrA*⁺ cells
17 (Figure 3A). In contrast, the *ezrA* null counterparts were fully viable in the presence of inducer
18 (Figure 3A). Of the four QNR patch mutants, those that were severely impaired in medial
19 localization (Figure 2B and Table 2) fully restored viability to cells in the presence of inducer.
20 On the other hand, the *ezrA(Q506A)* mutation only weakly suppressed the lethality associated
21 with MinCD overexpression (Figure 3A), consistent with its intermediate localization phenotype
22 (Figure 2B and Table 2).

1 To extend these data, we examined the ability of the QNR patch mutants to suppress the
2 heat sensitivity of a conditional *ftsZ* allele, *ftsZts*. At 45°C, *ftsZts* cells fail to form FtsZ rings or
3 septa, leading to an ~3000-fold reduction in viability (17). Loss of function mutations in *ezrA* or
4 other inhibitors of cell division restore FtsZ ring formation and viability to *ftsZts* cells at the
5 restrictive temperature (17, 31).

6 In confirmation of an active role for EzrA at midcell, loss of medial EzrA localization
7 correlated with suppression of *ftsZts* heat sensitivity. As expected, an *ezrA* null mutation fully
8 restored viability to *ftsZts* cells at the restrictive temperature (Figure 3B). The QNR patch
9 mutants that were most severely impaired in medial EzrA localization (Figure 2B and Table 2)
10 restored full viability to *ftsZts* cells at the restrictive temperature (Figure 3B). Conversely,
11 EzrA(Q506A), which exhibits an intermediate medial EzrA localization phenotype (Figure 2B
12 and Table 2) conferred variable levels of suppression that ranged from poor to near-*ezrA*-null
13 levels (note the relatively large error bar in Figure 3B). These results confirm the results of the
14 MinCD overexpression assay and are consistent with a model in which EzrA acts at midcell to
15 destabilize FtsZ assembly at this position.

17 **EzrA QNR patch mutants retain the ability to inhibit polar FtsZ ring formation.**

18 Aberrant, polar FtsZ ring formation is a hallmark of a loss-of-function mutation in *ezrA*
19 (17). Polar ring formation is most likely due to an increase in FtsZ stability that overcomes
20 MinCD activity at cell poles (19). The inability of EzrA QNR patch mutants to localize to
21 midcell and the concurrent stabilization of the medial FtsZ ring is therefore consistent with a
22 defect in EzrA's ability to inhibit FtsZ assembly throughout the cell. To test this possibility we
23 examined FtsZ ring formation in the three *ezrA* QNR mutants [*ezrA(N509A)*, *ezrA(R510A)* and

1 *ezrA(R510D)*] that showed the greatest reduction in medial EzrA-GFP localization (Figure 2B
2 and Table 2).

3 Remarkably, the three QNR patch mutants retained the ability to inhibit polar FtsZ ring
4 formation (Figure 4), despite the loss of medial localization (Figure 2). Consistent with previous
5 work, the frequency of polar FtsZ ring formation in *ezrA* null cells was 15-fold higher than wild
6 type (Figure 4B). Of the three QNR patch mutants, *ezrA(N509A)* and *ezrA(R510A)* cells
7 displayed FtsZ ring localization patterns that were indistinguishable from wild type.
8 *ezrA(R510D)* cells exhibited a mild (3.9-fold) increase in polar ring formation (Figure 4B).
9 However, this increase was not statistically significant by χ^2 analysis ($\alpha = 0.001$.) Together,
10 these data indicate that the loss of localization to midcell does not preclude EzrA's ability to
11 inhibit FtsZ assembly at cell poles.

12
13 **A purified EzrA QNR patch mutant inhibits FtsZ assembly *in vitro* comparably to wild**
14 **type EzrA.**

15 The simplest explanation for the reduced medial localization of EzrA QNR patch mutants
16 and their corresponding increase in FtsZ stabilization at this position would be a defect in the
17 EzrA-FtsZ interaction. However, the ability of the QNR patch mutants to inhibit polar FtsZ ring
18 formation suggests that the EzrA-FtsZ interaction is at least partially intact. To resolve this issue,
19 we examined the ability of EzrA(R510D) to inhibit FtsZ assembly *in vitro*. We chose this mutant
20 as it exhibited the greatest reduction in medial localization (Figure 2B and Table 2). For
21 purification purposes we constructed a 6XHis-tagged version of EzrA(R510D), substituting a
22 Thioredoxin moiety for its N-terminal transmembrane anchor [Thio-EzrA(R510D)]. Relative

1 levels of FtsZ assembly were measured in real time by 90° angle light scattering (23) in the
2 presence or absence of wild type Thio-EzrA or Thio-EzrA(R510D).

3 Consistent with previous results (8), the addition of 1 mM GTP to a reaction containing 5
4 μM purified FtsZ led to a rapid increase in light scattering, while the presence of 10 μM purified
5 Thio-EzrA decreased FtsZ light scattering by ~60% (Figure 5A). This result was typical for wild
6 type EzrA purified using the two-step protocol described in the Materials and Methods.
7 Strikingly, Thio-EzrA(R510D) inhibited FtsZ assembly to the same degree as its wild type
8 counterpart (Figure 5A), even at low concentrations (Figure 5B). These data indicate that Thio-
9 EzrA(R510D) is wild type with regard to its ability to interact with FtsZ *in vitro* and are
10 consistent with data indicating that QNR patch mutants interact with FtsZ *in vivo* to inhibit polar
11 FtsZ ring formation (Figure 4).

12
13 **Loss of medial EzrA localization leads to an increase in cell length that is independent of**
14 **polar ring formation.**

15 Cells lacking *ezrA* are longer than wild type cells (4, 14, 17). It has been suggested that
16 the increased size of *ezrA* null mutants results from a dilution of division components at midcell
17 due to the presence of extra FtsZ rings at cell poles (14). Alternatively, changes in FtsZ polymer
18 dynamics in the absence of EzrA activity at midcell may be responsible for increases in cell size.
19 In support of the latter model, *ezrA* null mutants are longer than wild type cells even under
20 conditions that do not support the formation of extra FtsZ rings (*i.e.* growth in minimal glucose
21 medium) (17).

22 To determine whether the loss of EzrA activity at midcell is the proximal cause of the
23 increase in cell length observed in *ezrA* null mutants, we measured the length of QNR patch

1 mutants in both nutrient-rich (LB) and nutrient-poor [S7₅₀-minimal glucose (13)] media. If EzrA
2 plays an active role at midcell, then *ezrA* QNR mutants should be longer than wild type cells
3 despite the low frequency of polar ring formation. Conversely, if the increased length of *ezrA*
4 null mutants is a consequence of extra FtsZ ring formation at cell poles, then *ezrA* QNR mutants
5 should exhibit a wild type cell length distribution.

6 Our data indicate that EzrA localization to midcell is essential for maintaining proper cell
7 size, regardless of polar FtsZ ring formation. Wild type cells cultured in LB had a mean length of
8 ~4.0 μm , while *ezrA* null cells were ~75% longer (mean ~7.0 μm). For the QNR mutants, cell
9 length (Figure 6) correlated with localization pattern (Figure 2 and Table 2). The two mutants
10 that displayed an intermediate EzrA localization phenotype [*ezrA(N509A)* and *ezrA(R510A)*]
11 both had an average length ~23% greater (mean ~4.9 μm) than wild type cells. *ezrA(R510D)*
12 mutants, which are completely defective in medial EzrA localization, were ~45% longer than
13 wild type cells (mean ~5.8 μm). Together, these data show a significant shift in cell length
14 distribution upon disruption of medial EzrA localization (Figure 6A), even when few polar rings
15 are present.

16 We next examined the length of wild type and *ezrA* mutant cells cultured in S7₅₀ minimal
17 glucose. This growth condition does not support the formation of extra FtsZ rings although *ezrA*
18 null mutant populations possess a low percentage of cells with single polar FtsZ rings (17). As
19 expected, wild type *B. subtilis* cells cultured in minimal media were substantially shorter than
20 their counterparts cultured in LB (27), averaging ~3.2 μm long. Although shorter than in LB,
21 *ezrA* null mutants cultured under these conditions were still ~59% longer than wild type (mean
22 ~5.0 μm). As in LB, *ezrA* QNR mutants grown in minimal media also showed a statistically
23 significant increase in cell length compared to the wild type strain. *ezrA(N509A)* and

1 *ezrA(R510A)* mutants were both ~6% longer than wild type (mean ~3.6 μm), and the more
2 severe *ezrA(R510D)* mutant was ~31% longer (mean ~4.2 μm). The intermediate length of the
3 *ezrA(R510D)* mutant in LB and minimal glucose (Figure 6) suggests that it retains some residual
4 activity at midcell, despite showing no medial EzrA localization by fluorescence microscopy
5 (Figure 2). The frequency of minicell formation in *ezrA* null mutants and *ezrA* QNR mutants was
6 less than 4% in both minimal glucose and LB (data not shown), thus polar septation events that
7 occur at the expense of binary fission are unlikely to be the explanation for increases in cell
8 length.

9 As further evidence of a disturbance in cell size homeostasis, the *ezrA* QNR mutants
10 exhibited an increase in the ratio of cell length to FtsZ rings (L/R ratio). Wild type cells exhibit
11 an L/R ratio of ~6.5 $\mu\text{m}/\text{ring}$ under a range of growth conditions (29). Conversely, the L/R of
12 *ezrA* null cells increased by ~31% (~8.5 $\mu\text{m}/\text{ring}$) after growth in LB, despite the presence of
13 extra FtsZ rings. Of the QNR mutants, *ezrA(N509A)* and *ezrA(R510A)* each had an ~7% increase
14 in the L/R ratio (~6.9 $\mu\text{m}/\text{ring}$) and *ezrA(R510D)* had an ~19% increase in L/R (~7.7 $\mu\text{m}/\text{ring}$).
15 Cell widths were statistically indistinguishable between wild type and *ezrA* mutant cells (data not
16 shown).

17 Importantly, the percentage of *ezrA* mutants that contain FtsZ rings was identical to wild
18 type cells (Figure 4), as was mass doubling time (data not shown). These data indicate that the
19 timing of FtsZ ring formation relative to cell birth and the duration of the Z-period are
20 unperturbed. If loss of medial EzrA activity were to affect either of these two parameters we
21 would have instead expected to see changes in FtsZ ring frequency in an *ezrA* null cell
22 population compared to wild type. This is counter to previous reports suggesting that FtsZ ring
23 constriction is delayed in *ezrA* null mutants during slow growth (14). The difference between our

1 results and those of Kawai *et al.* (14) may reflect differences in strain background, media, and/or
2 temperature [*e.g.* our measurements were done on cells cultured in liquid medium at 37°C
3 whereas Kawai *et al.* used slow-growing cells cultured on solid medium at 24°C (14)]. Together,
4 these data indicate that the increased length of *ezrA* mutant cells is due to loss of EzrA activity at
5 midcell rather than dilution of division components in the presence of extra FtsZ rings at cell
6 poles.

ACCEPTED

1 DISCUSSION

2 We have identified a conserved 7-residue patch (the QNR patch) in the C-terminus of
3 EzrA (Figure 1A and B) that is required for interaction with the preformed FtsZ ring. A single
4 substitution in the QNR patch abolishes medial EzrA localization (Figure 2), but does not alter
5 the ability of EzrA to inhibit FtsZ assembly *in vitro* (Figure 5) and results in only a modest
6 increase in polar FtsZ ring formation (Figure 4).

7 The isolation of *ezrA* mutants that are specifically defective for medial localization has
8 allowed us to clarify the role of EzrA at the cytokinetic ring. Notably, our data indicate that EzrA
9 contributes to FtsZ assembly dynamics within the medial ring, thereby helping to coordinate
10 division with cell growth and ensuring that cells are the proper length upon cytokinesis. QNR
11 patch mutants were resistant to overexpression of the MinCD division inhibitor (Figure 3) and
12 exhibited increases in cell length (Figure 6), consistent with stabilization of FtsZ assembly at
13 midcell. The increase in cell length is unlikely to be due to a reduction in the cytoplasmic pool of
14 division components, as *ezrA* QNR mutants exhibited a pattern of FtsZ ring formation that was
15 statistically indistinguishable from wild type cells. Moreover, we saw a similar increase in *ezrA*
16 null cell length in minimal media (Figure 6), a condition that does not support the formation of
17 extra FtsZ rings (17). It is possible that *ezrA* QNR mutants possess a higher percentage of large
18 FtsZ polymers even in the absence of extra FtsZ rings, a situation that might effectively sequester
19 components of the division apparatus away from midcell. However, this explanation seems
20 unlikely given the significant stabilization of FtsZ assembly at midcell in the *ezrA* QNR mutant
21 backgrounds.

22 The idea that EzrA destabilizes FtsZ assembly at midcell appears to conflict with FRAP
23 data indicating FtsZ turnover rates are identical in wild type and *ezrA* null mutant cells (1).

1 However, FRAP also shows that the half-life for an FtsZ subunit in the cytokinetic ring varies
2 significantly from 4 to 20 seconds, even in wild type cells (1). Thus, it is possible that the loss of
3 *ezrA* has a modest effect on subunit turnover that is undetectable by FRAP, yet sufficient to alter
4 the stability of the medial FtsZ ring. Alternatively, the loss of EzrA may stabilize the FtsZ ring in
5 a manner that does not significantly decrease subunit turnover itself, *e.g.* boosting nucleation
6 potential at midcell or increasing the number of polymers in the ring itself.

7 Our data indicating that the frequency of FtsZ ring formation and the duration of the Z-
8 period are unperturbed in *ezrA* mutant cells (Figure 4) argues against a model in which the
9 increase in cell length is due to changes in the timing of cytokinesis and/or in the persistence of
10 the FtsZ ring, as previously suggested (14). Instead, we favor a model in which the loss of EzrA
11 activity at midcell increases the stability of the medial FtsZ ring, rendering it resistant to the
12 factors responsible for coordinating division with cell size. This situation would be analogous to
13 the increase in FtsZ polymer stability that overcomes the activity of the MinCD complex at the
14 poles of *ezrA* null mutant cells (19).

15 Despite being defective in medial localization (Figure 2), EzrA QNR patch mutants are
16 near wild type with regard to their ability to inhibit aberrant FtsZ assembly at cell poles (Figure
17 4). These data indicate that QNR mutants have not lost the ability to interact with FtsZ,
18 consistent with our *in vitro* data (Figure 5). It remains formally possible that in the absence of
19 medial EzrA localization there is an increase in EzrA concentrations at the cell poles that
20 compensates for a decreased EzrA-FtsZ interaction, thus allowing inhibition of polar FtsZ
21 assembly to persist. However, EzrA(R510D), which is completely defective in medial
22 localization, inhibits FtsZ assembly *in vitro* to wild type levels (Figure 5), suggesting the EzrA-
23 FtsZ interaction remains robust.

1 Based on these results we propose that EzrA has at least two separate regions for
2 interaction with FtsZ. The first region, located in the N-terminal portion of EzrA, is required for
3 the interaction between EzrA and the free FtsZ monomers and multimers that constitute the
4 cytoplasmic pool of FtsZ. The second region, contained in the QNR patch, promotes interaction
5 with the single-stranded polymers and bundles that constitute the FtsZ ring, but is dispensable for
6 inhibition of *de novo* FtsZ assembly. Alternatively, the QNR patch may be required for
7 interaction between EzrA and another component of the cytokinetic ring, thereby bringing EzrA
8 into close proximity with FtsZ at this position. A fusion of the QNR patch to the C-terminus of
9 GFP was unable to localize to the FtsZ ring on its own, indicating that while necessary, it is not
10 sufficient for medial localization (DPH, unpublished data).

11 Together, our results support a model in which EzrA serves two distinct functions *in*
12 *vivo*: one in which it prevents aberrant FtsZ assembly at cell poles, as previously characterized
13 (8, 17, 19) and one in which it destabilizes FtsZ assembly at midcell, enhancing the dynamic
14 nature of the medial FtsZ ring and ensuring that division is coupled to cell growth. Future work
15 will address whether the QNR patch of EzrA is required for interaction with preformed FtsZ
16 polymers or for interaction with other division proteins. Our results highlight the need for a more
17 comprehensive understanding of the molecular nature of FtsZ interaction with its modulating
18 proteins, particularly those that appear to interact with FtsZ at more than one subcellular
19 location.

20

21

22

23

1 **ACKNOWLEDGMENTS**

2 The authors would like to thank P. Chivers, H. Erickson, and D. Rudner for the generous
3 gift of plasmids or strains and D. Gregg, N. Hill, R. Kranz, M. Oates Leslie, Q. Luo, L.
4 Romberg, and R. Weart for technical assistance, advice, and/or insightful comments on the
5 manuscript. We are also grateful to members of the Levin laboratory for useful discussions
6 during the course of this research.

7 This work was supported in part by a Public Health Services grant (GM64671) from the
8 NIH and a National Science Foundation CAREER award (MCB-0448186) to PAL. AZB was
9 funded in part by a Ruth L. Kirschstein National Research Service Award from the NIH (F32-
10 GM077828). ACG was funded in part by a summer undergraduate research fellowship from the
11 Howard Hughes Medical Institute.

ACCEPTED

12
13
14
15
16
17
18
19
20
21

1 **REFERENCES**

- 2 1. **Anderson, D. E., F. J. Gueiros-Filho, and H. P. Erickson.** 2004. Assembly dynamics
3 of FtsZ rings in *Bacillus subtilis* and *Escherichia coli* and effects of FtsZ-regulating
4 proteins. *J. Bacteriol.* **186**:5775-81.
- 5 2. **Benson, A. K., and W. G. Haldenwang.** 1993. Regulation of σ^B levels and activity in
6 *Bacillus subtilis*. *J. Bacteriol.* **175**:2347-2356.
- 7 3. **Chivers, P. T., and R. T. Sauer.** 1999. NikR is a ribbon-helix-helix DNA-binding
8 protein. *Protein Sci.* **8**:2494-500.
- 9 4. **Chung, K. M., H. H. Hsu, S. Govindan, and B. Y. Chang.** 2004. Transcription
10 regulation of *ezrA* and its effect on cell division of *Bacillus subtilis*. *J. Bacteriol.*
11 **186**:5926-32.
- 12 5. **Chung, K. M., H. H. Hsu, H. Y. Yeh, and B. Y. Chang.** 2006. Mechanism of
13 regulation of prokaryotic tubulin-like GTPase FtsZ by membrane protein EzrA. *J. Biol.*
14 *Chem.* **282**:14891-7.
- 15 6. **Errington, J., R. A. Daniel, and D. J. Scheffers.** 2003. Cytokinesis in bacteria.
16 *Microbiol. Mol. Biol. Rev.* **67**:52-65.
- 17 7. **Guzman, L. M., D. Belin, M. J. Carson, and J. Beckwith.** 1995. Tight regulation,
18 modulation, and high-level expression by vectors containing the arabinose P_{BAD}
19 promoter. *J. Bacteriol.* **177**:4121-4130.
- 20 8. **Haeusser, D. P., R. L. Schwartz, A. M. Smith, M. E. Oates, and P. A. Levin.** 2004.
21 EzrA prevents aberrant cell division by modulating assembly of the cytoskeletal protein
22 FtsZ. *Mol. Microbiol.* **52**:801-14.

- 1 9. **Hale, C. A., and P. A. J. d. Boer.** 1997. Direct binding of FtsZ to ZipA, an essential
2 component of the septal ring structure that mediates cell division in *E. coli*. *Cell* **88**:175-
3 185.
- 4 10. **Harry, E., L. Monahan, and L. Thompson.** 2006. Bacterial cell division: the
5 mechanism and its precision. *Int. Rev. Cytol.* **253**:27-94.
- 6 11. **Harwood, C. R., and S. M. Cutting (ed.).** 1990. *Molecular Biological Methods For*
7 *Bacillus*. John Wiley and Sons, Chichester.
- 8 12. **Ireton, K., D. Z. Rudner, K. J. Siranosian, and A. D. Grossman.** 1993. Integration of
9 multiple developmental signals in *Bacillus subtilis* through the Spo0A transcription
10 factor. *Genes & Dev.* **7**:283-294.
- 11 13. **Jaacks, K. J., J. Healy, R. Losick, and A. D. Grossman.** 1989. Identification and
12 characterization of genes controlled by the sporulation-regulatory gene *spo0H* in *Bacillus*
13 *subtilis*. *J. Bacteriol.* **171**:4121-4129.
- 14 14. **Kawai, Y., and N. Ogasawara.** 2006. *Bacillus subtilis* EzrA and FtsL synergistically
15 regulate FtsZ ring dynamics during cell division. *Microbiology* **152**:1129-41.
- 16 15. **Lemon, K. P., I. Kurtser, and A. D. Grossman.** 2001. Effects of replication termination
17 mutants on chromosome partitioning in *Bacillus subtilis*. *Proc. Natl. Acad. Sci. USA*
18 **98**:212-217.
- 19 16. **Levin, P. A.** 2002. Light microscopy techniques for bacterial cell biology, p. 115-132. *In*
20 P. J. Sansonetti and A. Zychlinsky (ed.), *Molecular Cellular Microbiology*. Academic
21 Press, Ltd., London.

- 1 17. **Levin, P. A., I. G. Kurtser, and A. D. Grossman.** 1999. Identification and
2 characterization of a negative regulator of FtsZ ring formation in *Bacillus subtilis*. Proc.
3 Natl. Acad. Sci. USA **96**:9642-7.
- 4 18. **Levin, P. A., and R. Losick.** 1996. Transcription factor Spo0A switches the localization
5 of the cell division protein FtsZ from a medial to a bipolar pattern in *Bacillus subtilis*.
6 Genes & Dev. **10**:478-488.
- 7 19. **Levin, P. A., R. L. Schwartz, and A. D. Grossman.** 2001. Polymer stability plays an
8 important role in the positional regulation of FtsZ. J. Bacteriol. **183**:5449-5452.
- 9 20. **Levin, P. A., J. J. Shim, and A. D. Grossman.** 1998. Effect of *minCD* on FtsZ ring
10 position and polar septation in *Bacillus subtilis*. J. Bacteriol. **180**:6048-6051.
- 11 21. **Margolin, W.** 2005. FtsZ and the division of prokaryotic cells and organelles. Nat. Rev.
12 Mol. Cell Biol. **6**:862-71.
- 13 22. **Marston, A. L., and J. Errington.** 1999. Selection of the midcell division site in
14 *Bacillus subtilis* through MinD-dependent polar localization and activation of MinC.
15 Mol. Microbiol. **33**:84-96.
- 16 23. **Mukherjee, A., and J. Lutkenhaus.** 1999. Analysis of FtsZ assembly by light scattering
17 and determination of the role of divalent metal cations. J. Bacteriol. **181**:823-32.
- 18 24. **Perego, M., G. B. Spiegelman, and J. A. Hoch.** 1988. Structure of the gene for the
19 transition state regulator *abrB*: regulator synthesis is controlled by the *spo0A* sporulation
20 gene in *Bacillus subtilis*. Mol. Microbiol. **2**:689-699.
- 21 25. **Romberg, L., and P. A. Levin.** 2003. Assembly dynamics of the bacterial cell division
22 protein FtsZ: poised at the edge of stability. Annu. Rev. Microbiol. **57**:125-54.

- 1 26. **Sambrook, J., E. F. Fritsch, and T. Maniatis.** 1989. *Molecular Cloning: A Laboratory*
2 *Manual*, 2nd ed. Cold Spring Harbor Laboratory Press, Cold Spring Harbor, N.Y.
- 3 27. **Sargent, M. G.** 1975. Control of cell length in *Bacillus subtilis*. *J. Bacteriol.* **123**:7-19.
- 4 28. **Singh, J. K., R. D. Makde, V. Kumar, and D. Panda.** 2007. A membrane protein,
5 EzrA, regulates assembly dynamics of FtsZ by interacting with the C-terminal tail of
6 FtsZ. *Biochemistry*. doi: 10.1021/bi700710j
- 7 29. **Weart, R. B., A. H. Lee, A. C. Chien, D. P. Haeusser, N. S. Hill, and P. A. Levin.**
8 2007. A metabolic sensor governing cell size in bacteria. *Cell* **130**:335-47.
- 9 30. **Weart, R. B., and P. A. Levin.** 2003. Growth rate-dependent regulation of medial FtsZ
10 ring formation. *J. Bacteriol.* **185**:2826-34.
- 11 31. **Weart, R. B., S. Nakano, B. E. Lane, P. Zuber, and P. A. Levin.** 2005. The ClpX
12 chaperone modulates assembly of the tubulin-like protein FtsZ. *Mol. Microbiol.* **57**:238-
13 49.
- 14 32. **Wu, L. J., and J. Errington.** 2004. Coordination of cell division and chromosome
15 segregation by a nucleoid occlusion protein in *Bacillus subtilis*. *Cell* **117**:915-25.
- 16
17
18
19
20
21
22
23
24

1 **FIGURE LEGENDS**

2 **FIGURE 1. EzrA contains a conserved patch of seven residues near its C-terminus. (A)** The

3 predicted domain structure of *B. subtilis* EzrA, drawn to scale. Numbers refer to amino acid
4 positions. EzrA consists of an amino-terminal transmembrane (TM) anchor, four cytoplasmic
5 coiled coil (CC) domains, and a C-terminal conserved residue patch. Transmembrane and coiled
6 coil predictions generated using the Simple Modular Architecture Research Tool (SMART)
7 (<http://smart.embl-heidelberg.de/>). **(B)** A segment of EzrA alignments across the low G-C Gram-
8 positive bacteria, highlighting the QNR patch. The fourth predicted coiled coil of *B. subtilis*
9 EzrA is given for orientation, but does not align precisely with the final coiled coil of other
10 EzrAs. **(C)** Schematic of EzrA mutants generated (with and/or without a GFP tag as indicated in
11 the text) to assess EzrA localization and activity *in vivo*. Boxes indicate point mutations in the
12 QNR patch.

14 **FIGURE 2. The QNR patch is required for EzrA localization to the FtsZ ring.** EzrA-GFP is

15 shown in green and cell membranes are shown in red. Scale bar = 5 μ m. Single headed arrows
16 denote strong localization, double-headed arrows denote weak localization, and heads alone (no
17 tail) highlight EzrA localization to septa. **(A)** Full-length EzrA-GFP localizes to the FtsZ ring
18 and cell membrane during exponential growth. C-terminal truncations that remove the QNR
19 patch abolish EzrA localization to the FtsZ ring, but do not affect membrane localization. **(B)**
20 Removal of, or substitutions in, the QNR patch disrupt EzrA localization to the FtsZ ring.

22 **FIGURE 3. Loss of medial EzrA localization stabilizes FtsZ assembly at midcell. (A)**

23 Suppression of the lethality associated with >12-fold MinCD overexpression. **(B)** Restoration of

1 viability to cells encoding the heat-sensitive *ftsZts* allele at the restrictive temperature of 45°C.
2 Error bars denote the standard deviation between a minimum of three replicate experiments.

3

4 **FIGURE 4. Disruption of medial localization does not interfere significantly with EzrA**
5 **ability to inhibit polar FtsZ ring formation.** (A) Immunofluorescence microscopy of fixed
6 cells stained for FtsZ (red) and cell wall (green). Scale bar = 5 μm. Arrows denote polar FtsZ
7 rings. (B) FtsZ localization patterns in wild type (white), *ezrA null* (black), *ezrA(N509A)* (light
8 gray), *ezrA(R510A)* (gray) and *ezrA(R510D)* (dark gray) cells.

9

10 **FIGURE 5. Purified Thio-EzrA(R510D) inhibits FtsZ assembly *in vitro* comparably to WT**
11 **Thio-EzrA.** (A) Representative traces of FtsZ assembly from 90° angle light scattering assays.
12 FtsZ + GTP (gray), FtsZ + Thio-EzrA + GTP (black), FtsZ + Thio-EzrA(R510D) + GTP (white).
13 FtsZ is at 5 μM, EzrAs are at 10 μM, and GTP is at 1 mM. (B) Thio-EzrA(R510D) (white)
14 inhibits 5 μM FtsZ assembly comparably to wild type Thio-EzrA (black) across a range of
15 concentrations. Error bars denote standard deviation between five replicate experiments.

16

17 **FIGURE 6. Loss of medial EzrA localization leads to an increase in cell length that is**
18 **independent of polar ring formation.** Cell length distribution of strains grown in (A) LB and
19 (B) minimal glucose media. Strains are as follows: Wild type (white), *ezrA null* (black),
20 *ezrA(N509A)* (light gray), *ezrA(R510A)* (gray) and *ezrA(R510D)* (dark gray).

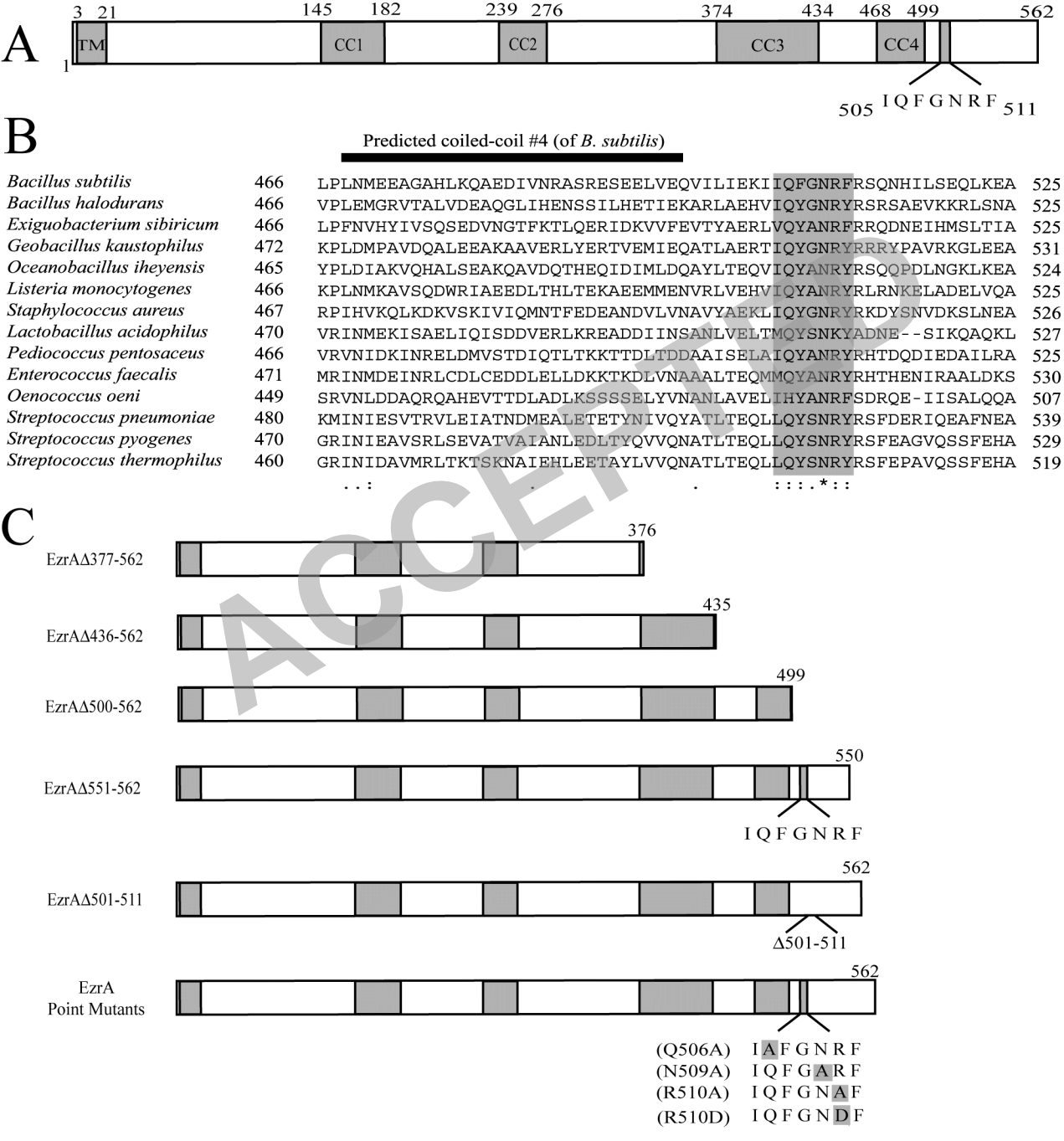
TABLE 1

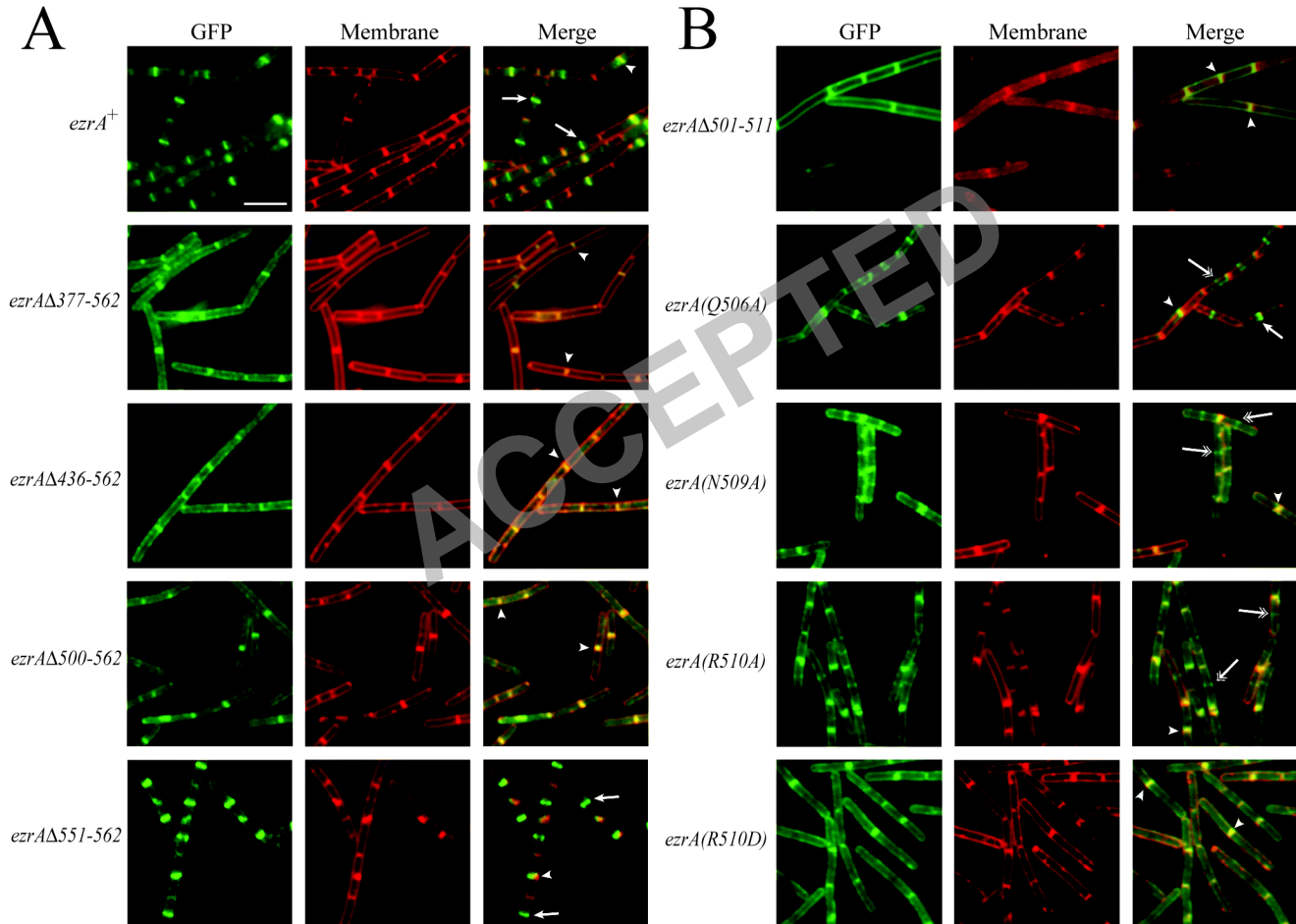
Strain	Genotype	Reference
JH642	<i>B. subtilis trpC2 pheA1</i>	(24)
PL847	<i>JH642 ezrA::ezrA-gfp spc</i>	(17)
PL872	<i>JH642 ezrA::ezrAΔ377-562-gfp spc</i>	This work
PL1626	<i>JH642 ezrA::ezrAΔ436-562-gfp spc</i>	This work
PL1628	<i>JH642 ezrA::ezrAΔ500-562-gfp spc</i>	This work
PL1630	<i>JH642 ezrA::ezrAΔ551-562-gfp spc</i>	This work
PL1693	<i>JH642 ezrA::ezrAΔ501-511-gfp spc</i>	This work
PL1718	<i>JH642 ezrA::ezrA(Q506A)-gfp spc</i>	This work
PL1719	<i>JH642 ezrA::ezrA(N509A)-gfp spc</i>	This work
PL1776	<i>JH642 ezrA::ezrA(R510D)-gfp spc</i>	This work
PL1900	<i>JH642 ezrA::ezrA(R510A)-gfp spc</i>	This work
PL867	<i>JH642 ezrA::spc</i>	(17)
PL1737	<i>JH642 ezrA::ezrA(Q506A) spc</i>	This work
PL1739	<i>JH642 ezrA::ezrA(N509A) spc</i>	This work
PL1780	<i>JH642 ezrA::ezrA(R510D) spc</i>	This work
PL1940	<i>JH642 ezrA::ezrA(R510A) spc</i>	This work
PL1145	<i>JH642 thrC::Pspachy-minCD erm</i>	(31)
MO45	<i>JH642 ezrA::kan</i>	This work
MO49	<i>JH642 thrC::Pspachy-minCD erm ezrA::kan</i>	This work
PL1749	<i>JH642 thrC::Pspachy-minCD erm ezrA::ezrA(Q506A) spc</i>	This work
PL1750	<i>JH642 thrC::Pspachy-minCD erm ezrA::ezrA(N509A) spc</i>	This work
PL1787	<i>JH642 thrC::Pspachy-minCD erm ezrA::ezrA(R510D) spc</i>	This work
PL1963	<i>JH642 thrC::Pspachy-minCD erm ezrA::ezrA(R510A) spc</i>	This work
PL642	<i>JH642 ftsZ::ftsZ-gfp cat</i>	(17)
PL876	<i>JH642 ftsZ::ftsZ-gfp cat ezrA::spc</i>	This work
PL1752	<i>JH642 ftsZ::ftsZ-gfp cat ezrA::ezrA(Q506A) spc</i>	This work
PL1753	<i>JH642 ftsZ::ftsZ-gfp cat ezrA::ezrA(N509A) spc</i>	This work
PL1827	<i>JH642 ftsZ::ftsZ-gfp cat ezrA::ezrA(R510D) spc</i>	This work
PL1971	<i>JH642 ftsZ::ftsZ-gfp cat ezrA::ezrA(R510A) spc</i>	This work
AG1111	<i>DZR200 = MC1061 F'lacIQ lacZM15 Tn10(Tet)</i>	(12)
ER2566	<i>F-λ-fhuA2 [lon] ompT lacZ::T7 gene 1 gal sulA11 Δ(mcrC-mrr) 114::IS10 R(mcr-73::miniTn10-TetS)2 R(zgb-210::Tn10)(TetS) endA1[dcm]</i>	(Lab stock)
PL1184	<i>ER2566 pBS58 pCXZ</i>	(8)
BB101	<i>slyD- lac pro F' (lacIq) ara, lacpro, nalA argEam (λDE3)</i>	(3)
PL1364	<i>BB101 pBAD Thio-EzrAΔTM-6XHis TOPO</i>	(8)
PL1821	<i>BB101 pBAD Thio-EzrAΔTM(R510D)-6XHis TOPO</i>	This work

TABLE 2

Strain	Strong Medial Localization	Weak Medial Localization	No Medial Localization
<i>ezrA-gfp</i>	63% (136/215)	16% (34/215)	21% (45/215)
<i>ezrA(Q506A)-gfp</i>	45% (123/272)	38% (102/272)	17% (47/272)
<i>ezrA(N509A)-gfp</i>	11% (25/227)	29% (66/227)	60% (136/227)
<i>ezrA(R510A)-gfp</i>	0% (0/317)	33% (105/317)	67% (212/317)
<i>ezrA(R510D)-gfp</i>	0% (0/136)	0% (0/136)	100% (136/136)

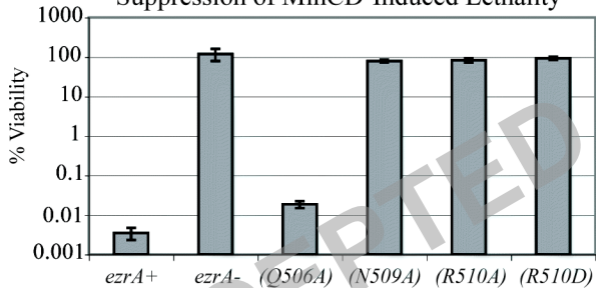
ACCEPTED



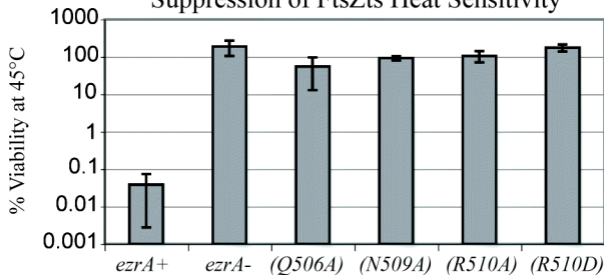


A

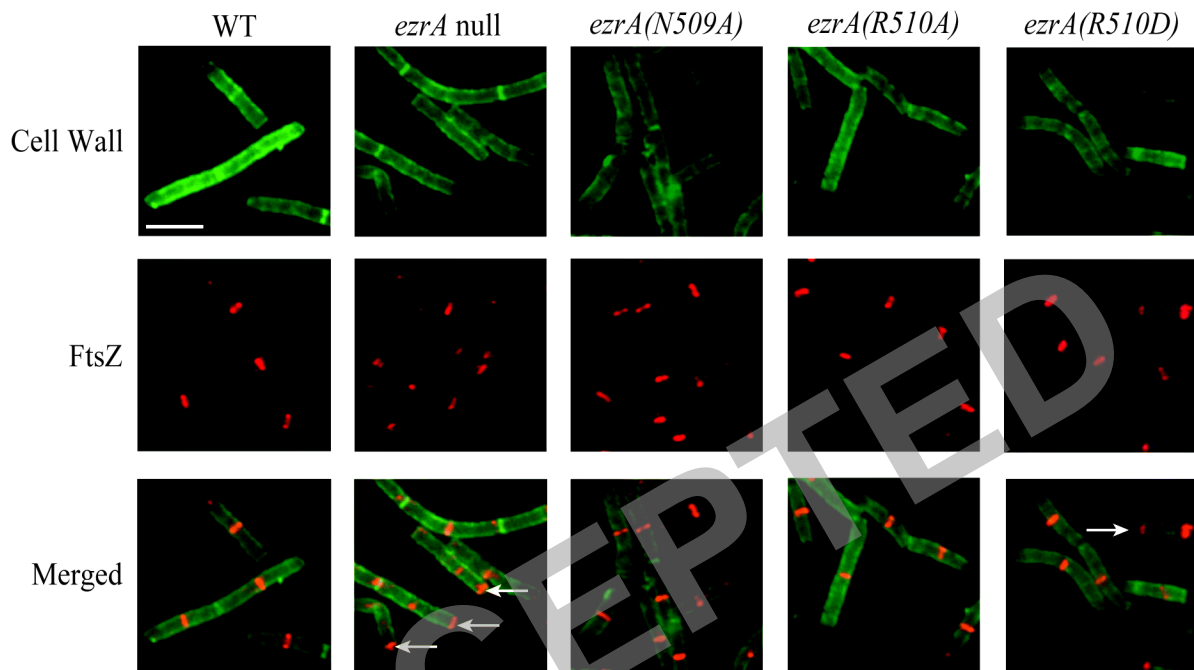
Suppression of MinCD-Induced Lethality

**B**

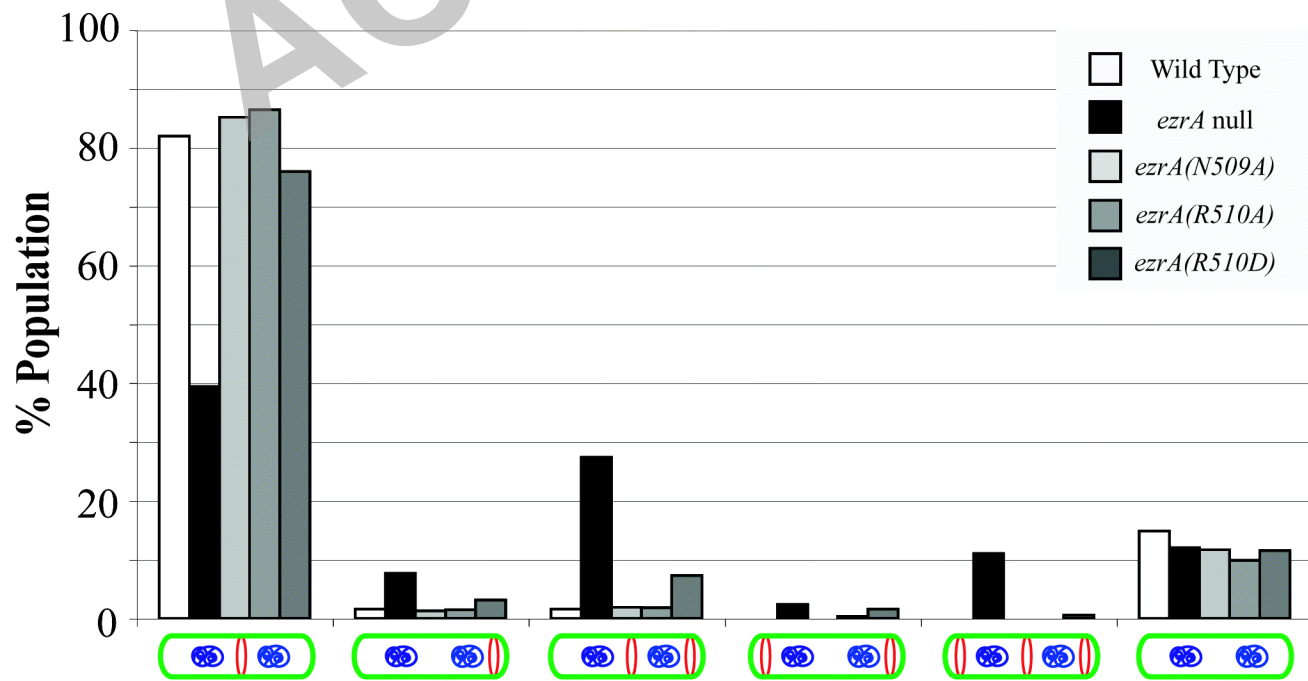
Suppression of FtsZts Heat Sensitivity

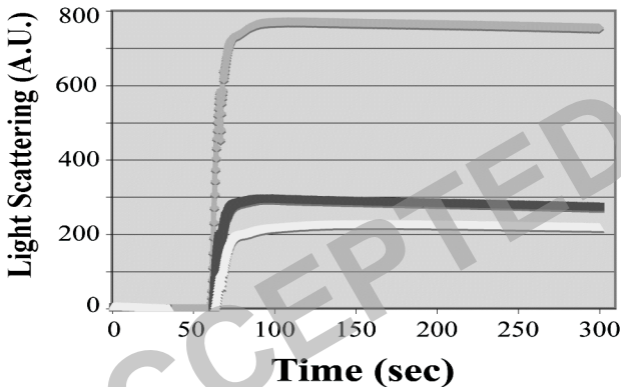
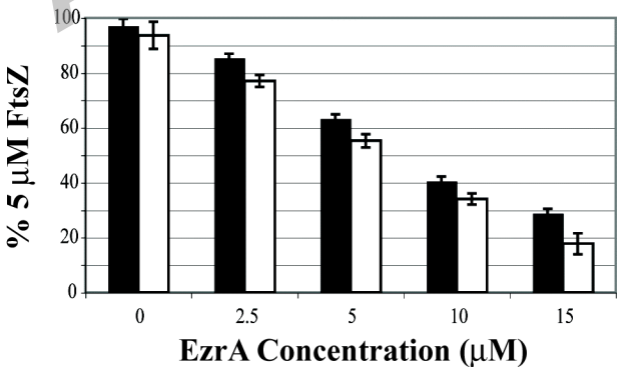


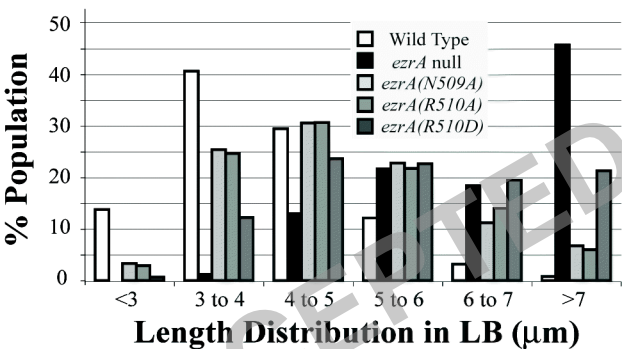
A



B



A**B**

A**B**